



Impact of Morphology in the Genotype and Phenotype Correlation of Bilateral Macronodular Adrenocortical Disease (BMAD): A Series of Clinicopathologically Well-Characterized 35 Cases

Florian Violon^{1,3} · Lucas Bouys^{1,2} · Annabel Berthon¹ · Bruno Ragazzon¹ · Maxime Barat¹ · Karine Perlemoine¹ · Laurence Guignat² · Benoit Terris³ · Jérôme Bertherat^{1,2} · Mathilde Sibony^{1,3}

Accepted: 12 January 2023 / Published online: 2 March 2023

© The Author(s), under exclusive licence to Springer Science+Business Media, LLC, part of Springer Nature 2023

Abstract

Bilateral macronodular adrenocortical disease (BMAD) is characterized by the development of adrenal macronodules resulting in a pituitary-ACTH independent Cushing's syndrome. Although there are important similarities observed between the rare microscopic descriptions of this disease, the small series published are not representative of the molecular and genetic heterogeneity recently described in BMAD. We analyzed the pathological features in a series of BMAD and determined if there is correlation between these criteria and the characteristics of the patients. Two pathologists reviewed the slides of 35 patients who underwent surgery for suspicion of BMAD in our center between 1998 and 2021. An unsupervised multiple factor analysis based on microscopic characteristics divided the cases into 4 subtypes according to the architecture of the macronodules (containing or not round fibrous septa) and the proportion of the different cell types: clear, eosinophilic compact, and oncocytic cells. The correlation study with genetic revealed subtype 1 and subtype 2 are associated with the presence of *ARMC5* and *KDM1A* pathogenic variants, respectively. By immunohistochemistry, all cell types expressed CYP11B1 and HSD3B1. HSD3B2 staining was predominantly expressed by clear cells whereas CYP17A1 staining was predominant on compact eosinophilic cells. This partial expression of steroidogenic enzymes may explain the low efficiency of cortisol production in BMAD. In subtype 1, trabeculae of eosinophilic cylindrical cells expressed DAB2 but not CYP11B2. In subtype 2, KDM1A expression was weaker in nodule cells than in normal adrenal cells; alpha inhibin expression was strong in compact cells. This first microscopic description of a series of 35 BMAD reveals the existence of 4 histopathological subtypes, 2 of which are strongly correlated with the presence of known germline genetic alterations. This classification emphasizes that BMAD has heterogeneous pathological characteristics that correlate with some genetic alterations identified in patients.

Keywords Bilateral macronodular adrenocortical disease · Adrenal · Adrenal nodular disease · Cushing · *ARMC5* · *KDM1A*

Introduction

Primary bilateral macronodular adrenal hyperplasia is a rare cause of Cushing's syndrome, first described in 1964 [1] with changing terminology over the years. The recent description of clonal molecular alterations has led to consider the neoplastic nature of the disease and the name BMAD for the bilateral macronodular adrenocortical disease was first proposed by Pakbaz and Mete [2] and then by Hodgson et al. and Juhlin et al. [3, 4] and endorsed by the WHO Adrenal Cortex Tumor Classification Consensus Conference 2022 [5].

BMAD is mainly diagnosed in patients in the 5th or 6th decade [6]. It is defined by the development of several bilateral macronodules larger than one centimeter. Some cases can be asymmetrical. This disease is also heterogeneous as

✉ Jérôme Bertherat
jerome.bertherat@aphp.fr

✉ Mathilde Sibony
mathilde.sibony@aphp.fr

¹ Université Paris-Cité, Institut Cochin, CNRS UMR8104, Inserm U1016, Paris, France

² Department of Endocrinology and National Reference Center for Rare Adrenal Disorders, Hôpital Cochin, Assistance Publique Hôpitaux de Paris, Paris, France

³ Department of Pathology, Hôpital Cochin, Assistance Publique Hôpitaux de Paris, Paris, France

demonstrated by the high variability in the clinical signs of Cushing's syndrome [7], the level of pituitary ACTH-independent hypercortisolism [8, 9], and the number of nodules seen on CT [7]. Steroidogenesis inhibitors (such as metopirone or ketoconazol) have been reported in some cases to control hypercortisolism, but adrenalectomy (bilateral or in selected cases unilateral) is the standard treatment indicated on the basis of the comorbidities and the level of cortisol excess [6, 8, 10].

In contrast with this clinical heterogeneity, to date, pathological descriptions are rather homogeneous in the 55 published case reports of BMAD including a pathological description. Indeed, the enlarged adrenal glands distorted by multiple yellow macronodules larger than 1 cm and up to more than 4 cm, well bounded by fibrous trabeculae appears as the main macroscopic description of BMAD. Stratakis and then Hsiao and collaborators proposed to divide BMAD into two subtypes, type I and II based on the presence of residual adrenal gland [11, 12]. Type I is characterized by nodules separated by residual adrenal gland while type II is characterized by no residual adrenal gland or atrophic cortex around the nodules. The nodules were composed of a majority of large, clear, lipid-rich, microvacuolated cells similar to those of the zona fasciculata. However, the proportion of smaller, eosinophilic compact cells was variable between cases [1, 13–45]. These observations support the hypothesis that a pathological heterogeneity could exist in BMAD.

Most cases are isolated. They can be sporadic or familial [7]. Indeed, rare BMAD cases have initially been described in patients with a genetic syndrome [4, 46] such as multiple endocrine neoplasia type 1 (*MEN1* gene) [4, 46–48], familial adenomatous polyposis (*APC* gene) [4, 46, 49], hereditary leiomyomatosis and renal cell cancer (*FH* gene) [4, 38, 46], and McCune Albright syndrome (*GNAS* gene) [4].

The recent molecular descriptions demonstrated a genetic heterogeneity in isolated BMAD. To date, these genetic studies divide the isolated BMAD into 3 genetic groups [50]. The first group presents with biallelic inactivation of the *ARMC5* (Armadillo containing protein 5) gene [51]. *ARMC5* pathological variants are found in about 20 to 25% of isolated BMAD cases [52, 53], 50% of the operated patients (due to more severe forms) [51, 54], and in 80% of cases with a familial presentation [7]. The second group presents with biallelic inactivation of the *KDM1A* (lysine (K)-specific demethylase 1A/LSD1) gene [50, 55]. The presence of this inactivation leads to aberrant expression of the GIP (gastric inhibitory polypeptide) receptor by the adrenal cortical cells, resulting in food-dependent hypercortisolism [19]. To date, the third group has no identified genetic alteration [50].

So far, no pathological classification of this clinically, molecularly, and genetically heterogeneous disease has been described. We propose the first study based on pathological characteristics and immunoexpression of adrenocortical markers in a large series of 35 BMAD. We then looked for potential correlations between the pathological features identified and the characteristics of the patients, in particular, their genotype.

Material and Methods

Patients

The series concerned 35 index cases with Cushing's syndrome who underwent surgery for BMAD at the Cochin Hospital Paris, France, between 1998 and 2021. All patients had a constitutional genetic profile study (COMETE network). Leucocyte DNA from BMAD patients has been sequenced for *ARMC5*, *KDM1A*, *APC*, *PRKACA*, *PRKARIA*, and *MEN1* genes by next-generation sequencing using the Ion Personal Genome Machine system (Ion Torrent, Thermo Fisher Scientific, USA) or a NextSeq 500 sequencer (Illumina). All clinical, biological, radiological, and pathological information were collected without the knowledge of the genetic data.

All patients gave their written consent for research purposes including genetic analysis in the national COMETE network. This project was approved as a monocentric retrospective study by the data protection office (bureau de la protection des données, registre d'enregistrement AP-HP) (number 20220221155734) and the CLEP, (comité local d'éthique des publications de l'hôpital Cochin) (number AAA-2022–08,019). It complies with the principles of the declaration of Helsinki.

Clinic and Biology

The following clinical information were collected: age, sex, weight, and height. The following biological results were collected: 24-h urinary free cortisol, plasma cortisol at 8:00 am, at midnight, after dexamethasone suppression, and testosterone levels.

Radiology

Computed tomography (CT) scans were available for review in 29/35 patients (83%). An abdominal radiologist (M.B) reported the following morphological criteria: maximal adrenal gland size, number of nodules, and spontaneous adrenal gland attenuation.

Pathology

Macroscopic photographs and stained slides were reviewed by two pathologists (FV, MS) in consensus, without knowledge of clinical, biological, radiological, and genetic data. The following macroscopic criteria were collected: adrenal weight, number and maximum nodule size, color, separate or coalescent nature of nodules, and presence of residual adrenal parenchyma (type I) or not (type II) [12].

A microscopic study was performed on all available nodules on 3 µm sections stained with a Tissue-Tek Prisma Plus automat (Sakura Finetek Europe BV; Zoeterwoude, The Netherlands). We reviewed a median of 10 H&E slides by the case (minimum: 4, maximum: 20). The microscopic criteria collected were architecture (round fibrous septa or sparse fibrous trabeculae inside macronodules, usually evaluated by reticulin [56, 57] or by Sirius red histochemistry [58], presence or absence of trabeculae, pseudoglandular aspects), type and proportion of cells (clear, compact, and oncocytic cells), inflammatory infiltrate, and adipocytic metaplasia.

Exhaustive immunohistochemical study was performed on dewaxed sections of 3 µm thickness on a Leica BOND-III System (Leica, Berlin, Germany). HIER (heat-induced epitope retrieval) treatment was performed for 20 min in a pH6 buffer solution (EDTA buffer, Bond Epitope Retrieval Solution 1, Leica, Berlin, Germany) for anti-CYP17A1 (clone HPA048533, diluted 1:800, Sigma Aldrich, Saint Louis, USA), anti-DAB2 (clone HPA028888, diluted 1:800, Sigma Aldrich, Saint Louis, USA) anti-CYP11B2 (clone 41-17B, diluted 1:500; Millipore, Frankfurt, Germany), and anti-KDM1A antibodies (clone ab-17721, diluted 1:400; Abcam, Boston USA). HIER treatment was performed for 20 min in pH9 buffer (EDTA buffer, Bond Epitope Retrieval Solution 2, Leica, Berlin, Germany) for anti-alpha inhibin (clone R1 IR058 ready to use, Dako, Santa Clara, USA), anti-HSD3B1 (clone WH0003283M1, diluted 1:8000, Sigma Aldrich, Saint Louis, USA), anti-HSD3B2 (clone SAB1402232, diluted 1:8000, Sigma Aldrich, Saint Louis, USA), and anti-CYP11B1 antibodies (clone 80-7, diluted 1:100, Millipore, Frankfurt, Germany). We performed double immunostaining using anti-HSD3B2 and anti-alpha inhibin antibody and with anti-CYP17A1 and anti-DAB2 antibody.

In the normal adult adrenal gland, HSD3B2 is expressed in the zona fasciculata and reticularis and has a lower expression in the zona glomerulosa [59, 60]. HSD3B1 is expressed in the three zones of the adrenal cortex [59, 60]. CYP17A1 is expressed in the zona fasciculata and the zona reticularis [59]. CYP11B1 is expressed in the zona fasciculata [59, 60]. DAB2 is expressed diffusely in the zona glomerulosa and CYP11B2 is expressed by aldosterone-secreting cells in the zona glomerulosa [60–62]. Alpha

inhibin is expressed in the zona reticularis and can be expressed in the zona fasciculata [60, 63].

Statistical Analyses

The multiple factor analysis was performed with all microscopic criteria using R software (version 4.0.5, R Core Team (2021). R: A language and environment for statistical computing. R Foundation for Statistical Computing, Vienna, Austria. URL <https://www.R-project.org/>.) with Factoshiny library. All microscopic criteria, qualitative and quantitative, had the same weight. Clustering was performed without pre-treatment with K-means or consolidation. Metric was Euclidian. Statistical analyses were performed using nonparametric tests appropriate for small numbers. Qualitative data were analyzed using Fisher exact test using R software (version 4.0.5). Quantitative data were analyzed using Kruskal–Wallis and Wilcoxon tests using R software (version 4.0.5).

Results

Patients

Most patients were female (66%), overweight (45%), or obese (20.5%). The median age was in the 6th decade (51.3 years). All patients had pituitary ACTH-independent clinical or subclinical Cushing's syndrome. CT scans showed enlarged, multinodular adrenal glands with a spontaneous density of less than 20 HU in most cases (88%). Demographic, clinical, biological, and radiological characteristics are presented in Table 1.

Macroscopic Characteristics

By definition, all 35 patients had multinodular adrenal glands that increased in weight and volume. The nodules were mainly coalescent (86%) and yellow (72%). Some nodules contained red or brown areas. Most patients presented with type II with atrophic or no adrenal parenchyma around the nodules (57%). All macroscopic features are presented in Table 2.

Microscopic Characteristics

The nodules were densely cellular, well-bounded, and separated by fibrous trabeculae that contained capillaries. Most of the cases (63%) showed round fibrous septa around several nests of adrenal cells inside nodules. The architecture within the nodules was nest-like.

In most cases (33/35; 94%), the main cell population was composed of polygonal clear cells with microvacuolized

Table 1 Cohort characteristics

Cohort characteristics ^a		
Clinical data^b	Sex	
	Female	23 (66%)
	Male	12 (34%)
	Age, year	51.3 (30–76)
	BMI	
	> 30	10/29 (34.5%)
	25–30	13/29 (45%)
	< 25	6/29 (20.5%)
	Adrenalectomy	
	Bilateral	22/35 (63%)
Unilateral	13/35 (37%)	
Biological data^c	Cushing syndrome	
	Clinical	23/33 (70%)
	Subclinical	10/33 (10%)
	24 h free urinary cortisol/maximum normal value	2.71 (0.15–10.7)
	Plasma free cortisol after 1 mg dexamethasone, nmol/L	428.5 (62–1140)
	Plasma free cortisol 8 h, nmol/L	488.6 (196–1192)
	ACTH, pg/ml	0.2 (0–6)
CT scan data^d	Adrenal mean length, mm	49.5 (25–85)
	Number of nodules	8.4 (2–27)
	Maximum nodule size, mm	27.5 (10–51)
	HU without IV	
	< 20	22/25 (88%)
	> 20	3/25 (12%)

^aQuantitative data are presented as means with minimum and maximum value. Qualitative data are presented as ratio and percentage

^bSex, age, and adrenalectomy side data were available for all patients. BMI data were available for 29 patients

^cCushing syndrome and CLU/ULN data were available for 33 patients. Plasma cortisol after 1 mg dexamethasone was available for 28 patients. Plasma cortisol at 8 A.M was available for 32 patients. ACTH data were available for 31 patients

^dAdrenal mean length and nodule number were available for 28 patients. Maximum nodule size data were available for 23 patients. HU without IV data were available for 25 patients

cytoplasm and a medium-sized, round centrally located nucleus. Their proportion varied from 60 to more than 90% except for 2 cases with only 20% of clear cells.

In all cases, there were compact eosinophilic cells of smaller size. They were polygonal, regular with the cytoplasm of variable abundance, and a medium-sized, round centrally located nucleus. Their proportion varied from less than 10% to 40%. They were organized in islands, bands, or sheets intermingled with clear cells. In 11 cases, different cylindrical compact eosinophilic cells forming trabeculae were observed especially at the periphery of the nodules, close to the adipose tissue.

Occasionally, there were large, polygonal, oncocyctic cells with a round, nucleolated, eccentric nucleus. Their cytoplasm was abundant, strongly eosinophilic, and granular. These cells frequently demonstrated a marked

anisocytosis and anisokaryosis. Their proportion varied from less than 10% to 80%.

Most cases had an inflammatory lymphocytic infiltrate (63%) and adipocytic metaplasia (63%). Some cases had pseudoglandular aspects (cavitations in the center of several nests) of clear cells (29%). In one patient (3%), there was a myelolipomatous territory. All microscopic features are presented in Table 3.

Morphological Subtypes

We used all microscopic criteria listed in Table 4 to perform an unsupervised multiple-factor analysis. This analysis subdivided the 35 patients of our cohort into 4 distinct subtypes (Fig. 1).

Table 2 Macroscopic characteristics

Pathological characteristics ^a	Cohort
Macroscopic data ^b	
Adrenal mean weight (g)	48.4 (13.9–100)
Maximum nodule size (cm)	3.32 (1–8)
Nodule number	7.7 (2–27)
Nodule color	
Yellow	20/28 (72%)
Yellow with light brown areas	4/28 (14%)
Yellow with red to dark brown areas	4/28 (14%)
Nodule aspect	
Coalescent	24/28 (86%)
Separate	4/28 (14%)
Non nodular adrenal gland	
Yes (type I)	12/28 (43%)
No (type II)	16/28 (57%)

^aQuantitative data are presented as means with minimum and maximum value. Qualitative data are presented as ratio and percentage

^bAdrenal mean weight data were available for 34 patients. Maximum nodule size data were available for all 35 patients. Nodule aspect, color, and non-nodular adrenal gland data were available for 28 patients

Those subtypes showed specific macroscopic (Fig. 2) and microscopic (Figs. 3–7) characteristics that are presented in Table 5.

In subtype 1 ($n = 17$), macroscopically, the adrenal parenchyma was distorted by coalescent, yellow macronodules. Areas of residual non-nodular adrenal gland were rare (type II) (Fig. 2a, e). Microscopically, the macronodules contained round fibrous septa composed of collagen fibers (Fig. 3a, e, i) well demonstrated by reticulin and sirius red histochemistry. Clear cells occupied 70 to 90% of the nodules. Their size and shape were regular. Compact cells represented 10 to 30% of the nodules and formed islands or bands at the periphery and in the center of the nodules (Fig. 4a, e, i). Pseudoglandular aspects inside nodules and trabeculae of cylindrical eosinophilic cells at the periphery and toward the center of the nodules were only seen in this subtype (Fig. 5). Oncocytic cells were rare. Most cases did not show a lymphocytic infiltrate. Areas of adipocytic metaplasia were common (Fig. 4a, e).

In subtype 2 ($n = 4$), macroscopically, the adrenal gland was predominantly occupied by coalescent yellow nodules with some light brown areas. Most often, areas of residual non-nodular adrenal gland persisted (Fig. 2b, f). Microscopically, the macronodules contained round fibrous septa composed of collagen fibers (Fig. 3b, f, j). Clear cells occupied 60 to 70% of the nodules (Fig. 4b, f, j). Their size and shape were irregular (Fig. 6). Compact eosinophilic cells had abundant cytoplasm and represented 30 to 40% of the

Table 3 Microscopic characteristics

Pathological characteristics ^a	Cohort
Microscopic data ^b	
Round fibrous septa inside macronodules	
Yes	22/35 (63%)
No	13/35 (37%)
Trabeculae	
Yes	11/35 (31%)
No	24/35 (69%)
Clear cells proportion	
> 90%	9/35 (26%)
70 to 90%	17/35 (49%)
60 to 70%	4/35 (11%)
20 to 60%	5/35 (14%)
Compact cells proportion	
30 to 40%	4/35 (11%)
10 to 30%	17/35 (49%)
< 10%	14/35 (40%)
Oncocytic cells proportion	
40 to 80%	5/35 (14%)
< 40%	30/35 (86%)
Pseudoglandular aspect	
Yes	10/35 (29%)
No	25/35 (71%)
Lymphocytic infiltration	
Yes	21/35 (60%)
No	14/35 (40%)
Adipocytic metaplasia	
Yes	22/35 (63%)
No	13/35 (37%)

^aQuantitative data are presented as means with minimum and maximum value. Qualitative data are presented as ratio and percentage

^bMicroscopic data were available for all patients

nodules (Figs. 4b, f, and 6). They were organized in extensive sheets closely intermingled with clear cells. Oncocytic cells were rare. All cases had a lymphocytic infiltrate. Most cases had areas of adipocytic metaplasia. One of the 4 patients had a myelolipomatous territory.

Table 4 Microscopic criteria used for multiple factorial analysis

Quantitative criteria	Clear cells (%) Compact cells (%) Oncocytic cells (%)
Qualitative criteria	Round fibrous septa inside macronodules Trabeculae of cylindrical eosinophilic cells Pseudoglandular aspects Lymphocytic infiltration Adipocytic metaplasia

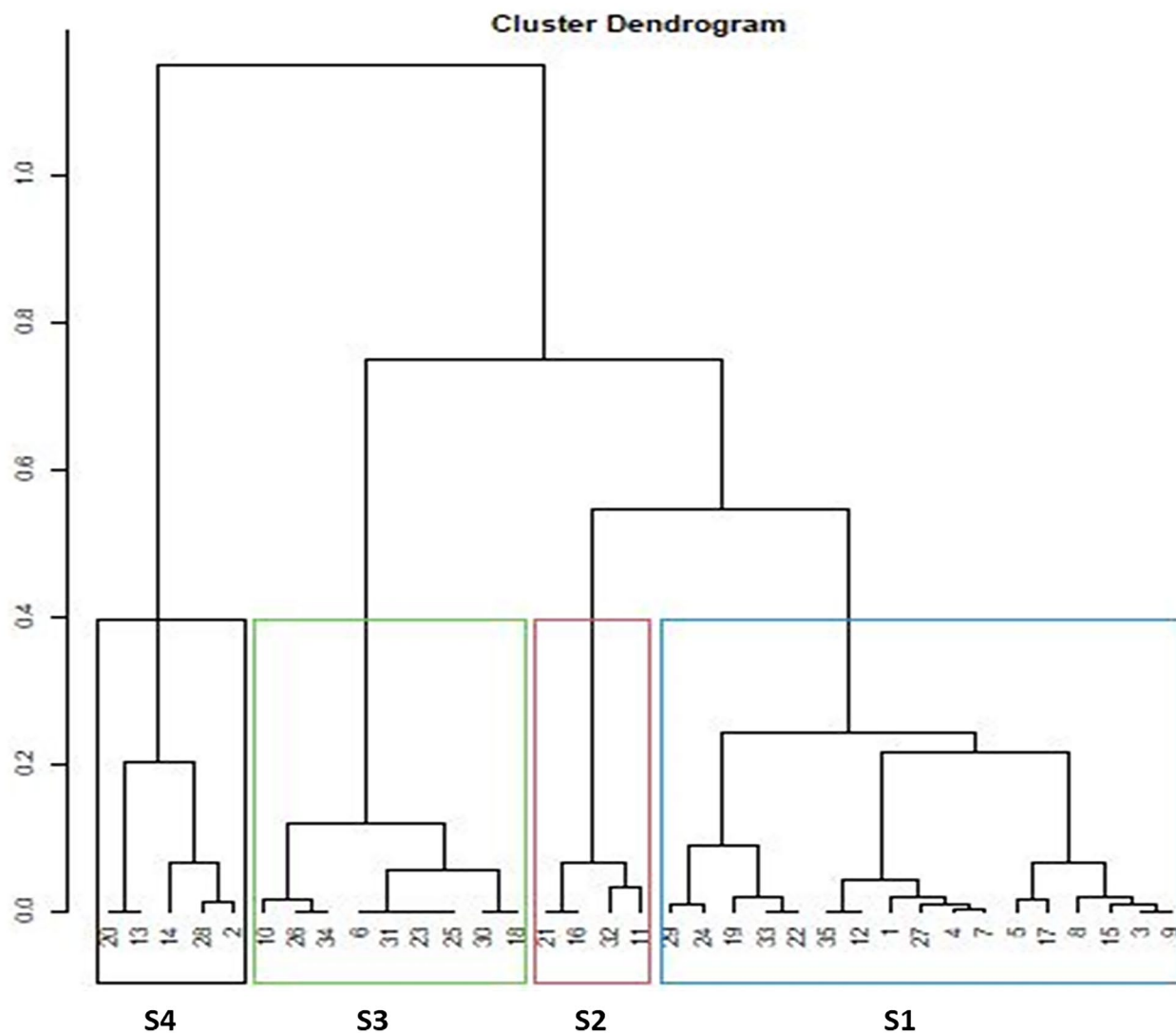


Fig. 1 Clustering divides the 35 BMAD cases into 4 morphological groups. S1, subtype 1; S2, subtype 2; S3, subtype 3; S4, subtype 4

In subtype 3 ($n=9$), the adrenal glands were occupied by large, coalescent, yellow nodules. The residual non-nodular adrenal gland was sometimes visible (Fig. 2c, g). Microscopically, the macronodules contained sparse arciform fibrosis (Fig. 3c, g, k). Clear cells occupied more than 90% of the nodules. Their size and shape were regular. Compact cells were uncommon and formed rare small nests scattered in the nodules. Oncocytic cells were rare. Most cases showed a lymphocytic infiltrate and areas of adipocytic metaplasia (Fig. 4c, g, k).

In subtype 4 ($n=5$), macroscopically, nodules were separated by areas of the non-nodular adrenal gland. The nodules were yellow and brown (Fig. 2d, h). Microscopically, the macronodules included sparse arciform fibrosis

(Fig. 3d, h, l). Oncocytic cells represented 40 to 80% of the nodules (Fig. 7). The proportion of clear cells varied between 20 and 60%. They were regular in size and shape. Compact cells were rare and formed small islands at the periphery or in the center of the nodules. Most cases had a lymphocytic infiltrate and adipocytic metaplasia (Fig. 4d, h, l).

Interestingly, this subtype classification concerned both adrenal glands when patients had a bilateral adrenalectomy. The presence of round fibrous septa inside nodules and the proportion of cells (i.e., clear, compact, and oncocytic) were the most discriminating criteria to distinguish these 4 subtypes (Table 6).

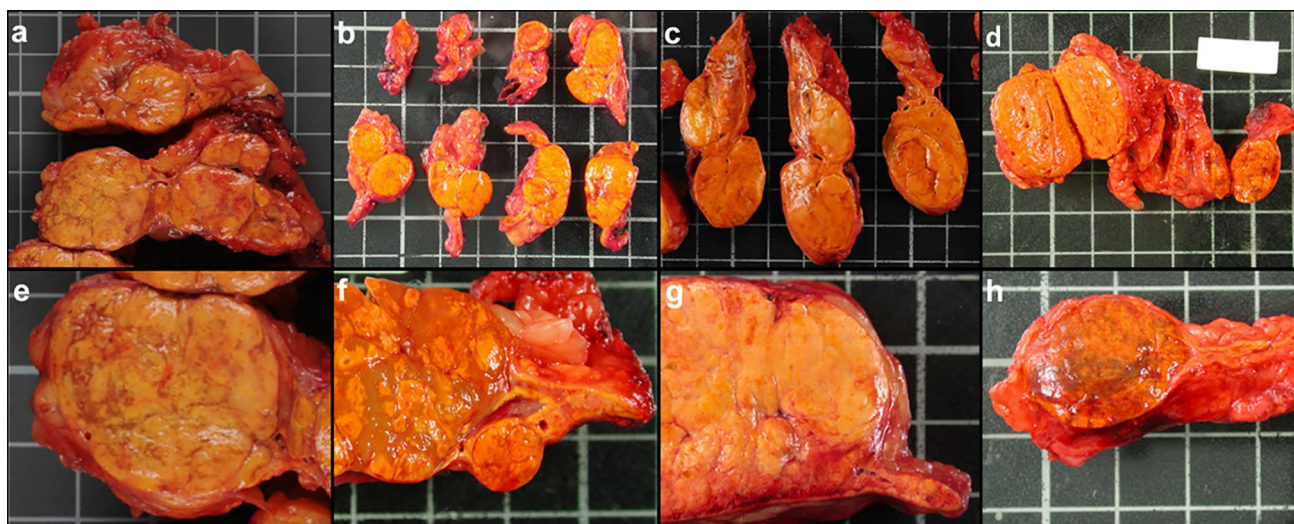


Fig. 2 Macrophotographs of BMAD. 1 white square=1 cm. Subtype 1 cases (a, e) had no non-nodular adrenal gland in contrast with other subtypes. Subtype 2 cases (b, f) showed a light brown area. Subtype 3 cases

(c, g) were composed of homogeneous yellow nodules. Subtype 4 cases (d, h) were made of dark brown nodules separated by the non-nodular adrenal

Immunohistochemistry

Immunohistochemical studies were performed on 34 out of 35 patients (Figs. 8, 9, 10, 11). The remaining patient had non-contributive results due to technical problems.

In all cases, HSD3B2 was preferentially expressed by clear cells (Fig. 8b–e, g–j). Fifteen cases (14 subtypes 1 and 1 subtype 3) showed diffuse staining on all clear cells (Fig. 8g). The remaining 19 cases showed heterogeneous staining with 40–80% of clear cells expressing HSD3B2

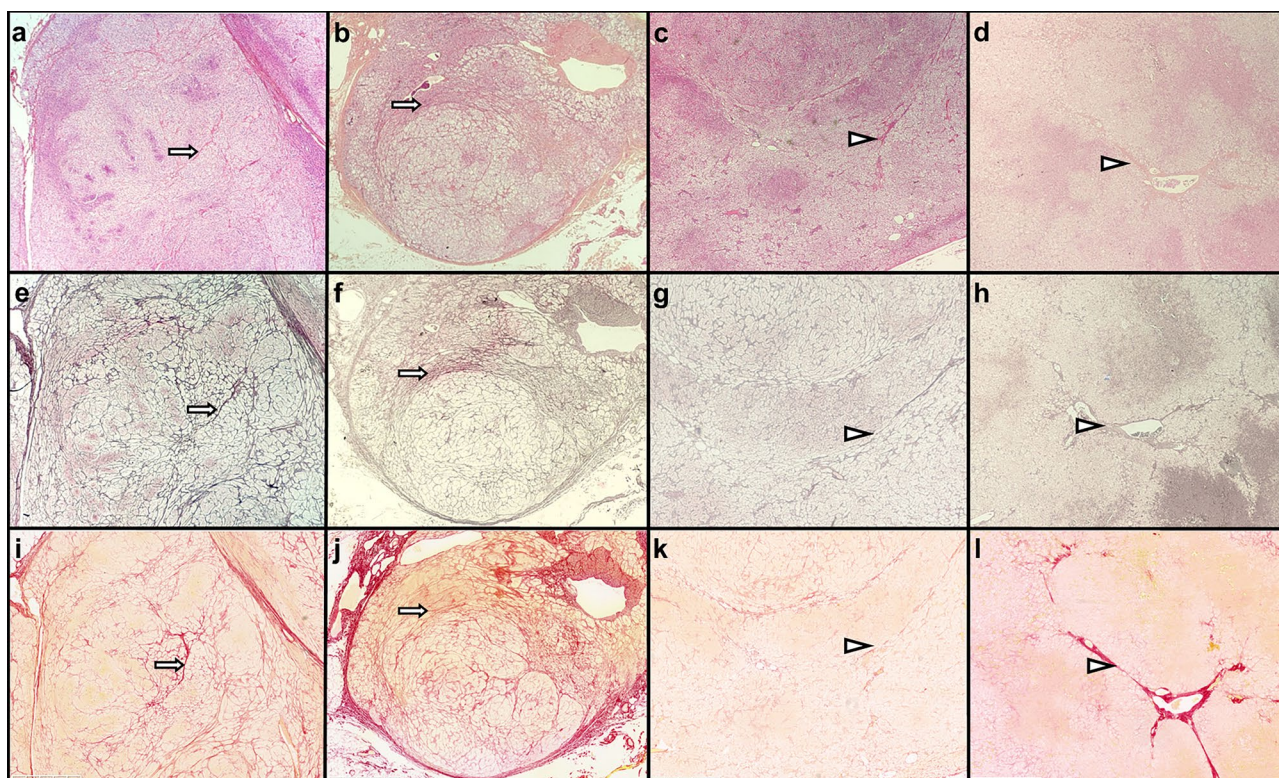


Fig. 3 Microphotographs of BMAD subtypes, H&E (a–d), reticulin histochemistry (e–h), and Sirius red histochemistry (i–l) magnification×25. Subtypes 1 (a, e, i) and 2 (b, f, j) cases had round fibrous septa within the

macronodules (arrow). Subtype 3 (c, g, k) and 4 (d, h, l) contained few sparse arciform fibrous trabeculae (arrowhead)

Table 5 Pathological characteristics of the subtypes

Pathological characteristics ^a	Subtype 1	Subtype 2	Subtype 3	Subtype 4	Total	<i>p</i>
Macroscopic data^b						
Adrenal mean weight (g)	51.8 (23–97.5)	39.9 (18.1–76.8)	62.2 (29.1–100)	22.4 (13.9–43)	48.4 (13.9–100)	0.015*
Maximum nodule size (cm)	3.2 (1–5)	3.6 (3–4.7)	4 (2–8)	2.6 (2–3)	3.32 (1–8)	0.45
Nodule number	11.5 (2–27)	4.7 (4–5)	6 (3–13)	2.7 (2–5)	7.7 (2–27)	0.04*
Nodule color						<0.0001*
Yellow	12/12 (100%)	0/4 (0%)	8/8 (100%)	0/4 (0%)	20/28 (72%)	
Yellow with light brown areas	0/12 (0%)	4/4 (100%)	0/8 (0%)	0/4 (0%)	4/28 (14%)	
Yellow with red to dark brown areas	0/12 (0%)	0/4 (0%)	0/8 (%)	4/4 (100%)	4/28 (14%)	
Nodule aspect						<0.0001*
Coalescent	12/12 (100%)	4/4 (100%)	8/8 (100%)	0/4 (0%)	24/28 (86%)	
Separate	0/12 (0%)	0/4 (0%)	0/8 (%)	4/4 (100%)	4/28 (14%)	
Non nodular adrenal gland						0.002*
Yes (type I)	1/12 (8%)	3/4 (75%)	4/8 (50%)	4/4 (100%)	12/28 (43%)	
No (type II)	11/12 (92%)	1/4 (25%)	4/8 (50%)	0/4 (0%)	16/28 (57%)	
Microscopic data^c						
Round fibrous septa inside macronodules						<0.0001*
Yes	17/17 (100%)	4/4 (100%)	0/9 (0%)	0/5 (0%)	22/35 (63%)	
No	0/17 (0%)	0/4 (0%)	9/9 (100%)	5/5 (100%)	13/35 (37%)	
Trabeculae						0.0004*
Yes	11/17 (65%)	0/4 (0%)	0/9 (0%)	0/5 (0%)	11/35 (31%)	
No	6/17 (35%)	4/4 (100%)	9/9 (100%)	5/5 (100%)	24/35 (69%)	
Clear cells proportion						<0.0001*
> 90%	0/17 (0%)	0/4 (0%)	9/9 (100%)	0/5 (0%)	9/35 (26%)	
70 to 90%	17/17 (100%)	0/4 (0%)	0/9 (0%)	0/5 (0%)	17/35 (49%)	
60 to 70%	0/17 (0%)	4/4 (100%)	0/9 (0%)	0/5 (0%)	4/35 (11%)	
20 to 60%	0/17 (0%)	0/4 (0%)	0/9 (0%)	5/5 (100%)	5/35 (14%)	
Compact cells proportion						<0.0001*
30 to 40%	0/17 (0%)	4/4 (100%)	0/9 (0%)	0/5 (0%)	4/35 (11%)	
10 to 30%	17/17 (100%)	0/4 (0%)	0/9 (0%)	0/5 (0%)	17/35 (49%)	
< 10%	0/17 (0%)	0/4 (0%)	9/9 (100%)	5/5 (100%)	14/35 (40%)	
Oncocytic cells proportion						<0.0001*
40 to 80%	0/17 (0%)	0/4 (0%)	0/9 (0%)	5/5 (100%)	5/35 (14%)	
< 40%	17/17 (100%)	4/4 (100%)	9/9 (100%)	0/5 (0%)	30/35 (86%)	
Pseudoglandular aspect						0.002*
Yes	10/17 (59%)	0/4 (0%)	0/9 (0%)	0/5 (0%)	10/35 (29%)	
No	7/17 (41%)	4/4 (100%)	9/9 (100%)	5/5 (100%)	25/35 (71%)	
Lymphocytic infiltration						0.03*
Yes	6/17 (35%)	4/4 (100%)	7/9 (88%)	4/5 (80%)	21/35 (60%)	
No	11/17 (65%)	0/4 (0%)	2/9 (22%)	1/5 (20%)	14/35 (40%)	
Adipocytic metaplasia						0.95
Yes	11/17 (65%)	3/4 (75%)	5/9 (56%)	3/5 (60%)	22/35 (63%)	
No	6/17 (35%)	1/4 (25%)	4/9 (44%)	2/5 (40%)	13/35 (37%)	

^aQuantitative data are presented as means with minimum and maximum value. Qualitative data are presented as ratio and percentage

^bAdrenal mean weight data were available for 34 patients. Maximum nodule size data were available for all 35 patients. Nodule aspect, color, and non-nodular adrenal gland data were available for 28 patients

^cMicroscopic data were available for all patients

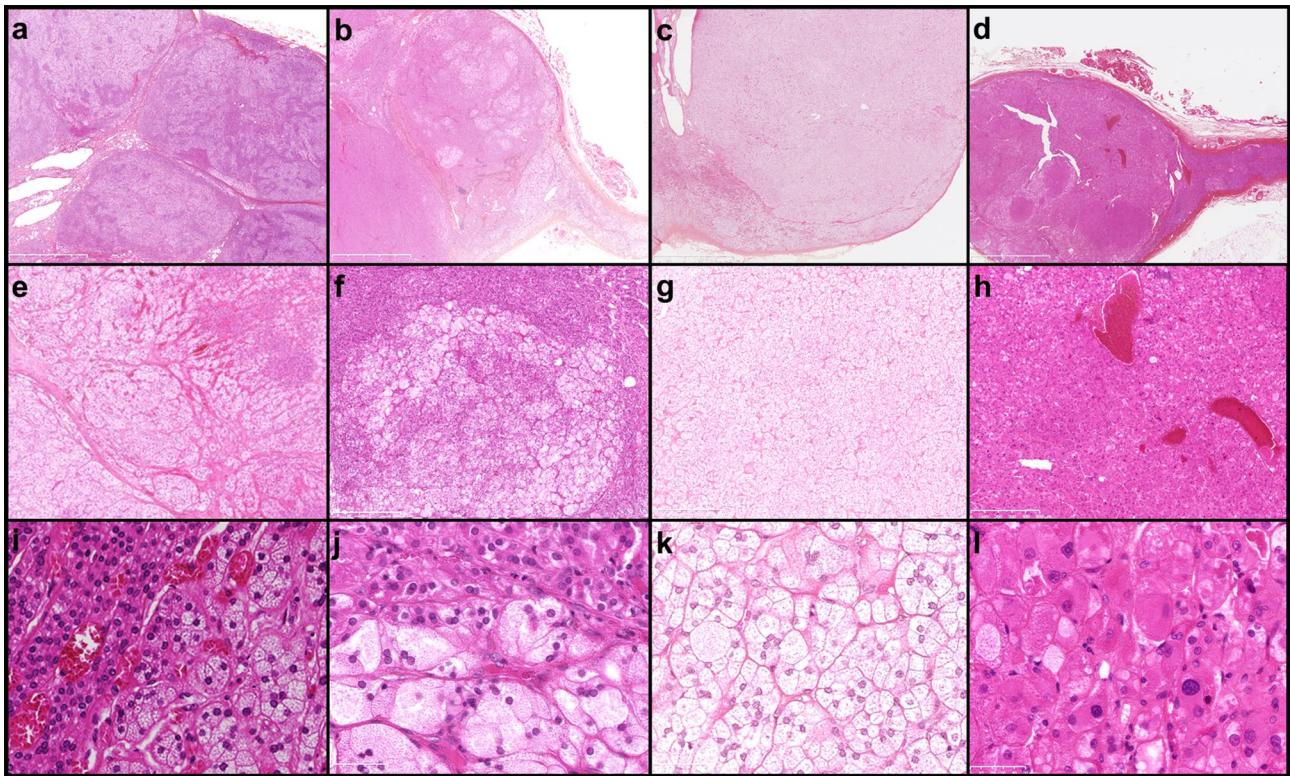


Fig. 4 Microphotographs of BMAD subtypes, H&E staining, magnification $\times 12.5$ (a–d), magnification $\times 50$ (e–h), and magnification $\times 400$ (i–l). Subtype 1 (a, e, i). Subtype 2 (b, f, j). Subtype 3 (c, g, k). Subtype 4 (d, h, l)

(Fig. 8h–j). In all cases, CYP17A1 was preferentially expressed in compact eosinophilic cells (Fig. 8b–e, l–o). HSD3B1 and CYP11B1 were expressed by all nodular cells, regardless of their type (Fig. 9).

DAB2 was expressed by peripheral trabecular cylindrical eosinophilic cells, only seen in subtype 1 (Fig. 10e). These

cells also express HSD3B2 but did not express CYP17A1 or CYP11B2 (Fig. 10f).

Alpha inhibin was preferentially expressed in islands and bands of polygonal compact cells. It was more abundant in subtype 2 than in the other subtypes (Fig. 8g–j).

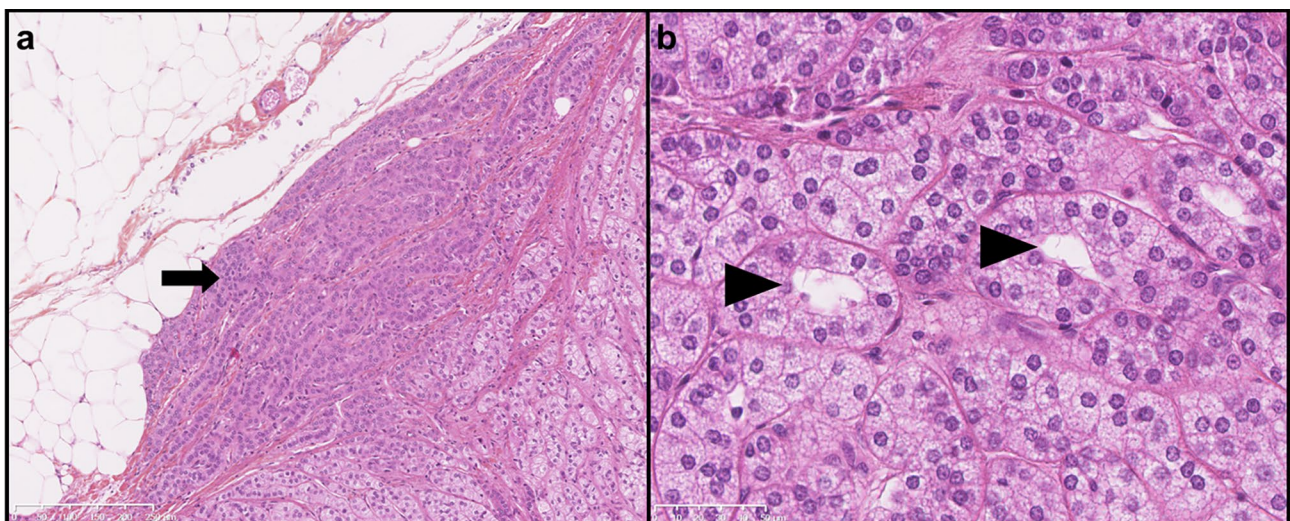


Fig. 5 Microphotograph of subtype 1 specificities, H&E staining. Eosinophilic cylindrical cells forming trabeculae at the periphery (arrow), magnification $\times 100$ (a). Pseudoglandular aspects with optically empty

cavitations in the center of clear cell nests (arrowhead), magnification $\times 400$ (b)

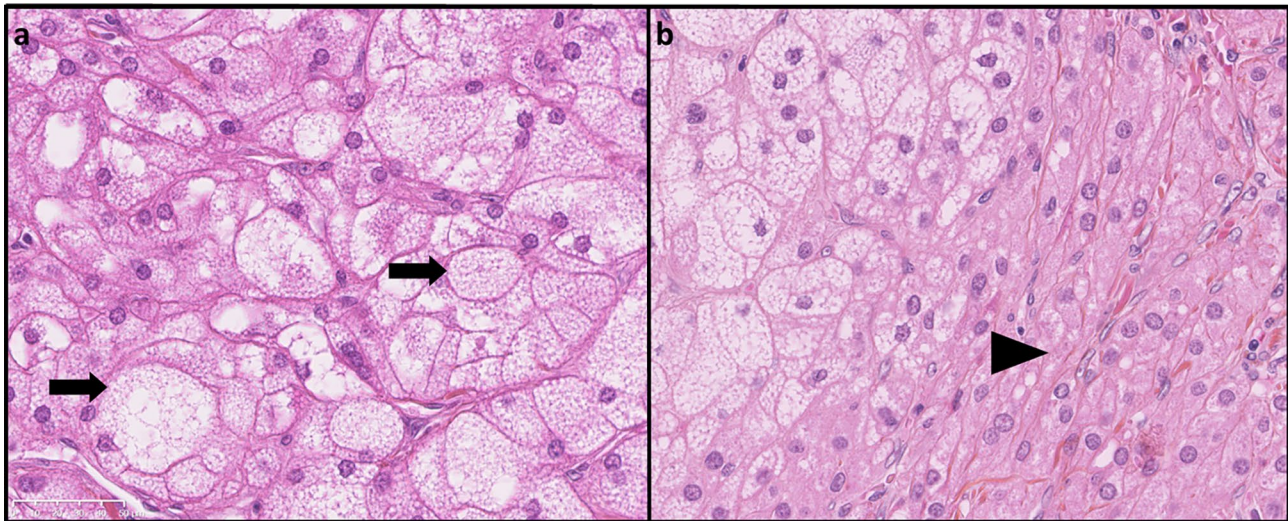


Fig. 6 Microphotograph of subtype 2 specificities, H&E staining. Clear cells irregular in size and shape (arrow), magnification $\times 400$ (a). Compact eosinophilic cells with abundant cytoplasm (arrowhead), magnification $\times 400$ (b)

KDM1A expression was weaker only in subtype 2 nodules (Fig. 11).

The oncocytic cells took up anti-HSD3B2, CYP17A1, and anti-alpha inhibin antibodies (Fig. 8e, j, o).

In cases where it was visible, the non-nodular adrenal showed an immunohistochemical profile similar to the one observed in a normal adrenal.

In summary, in all subtypes, HSD3B2 was mainly expressed by clear cells and CYP17A1 preferentially stained compact cells. HSD3B1 and CYP11B1 were expressed in all cell types.

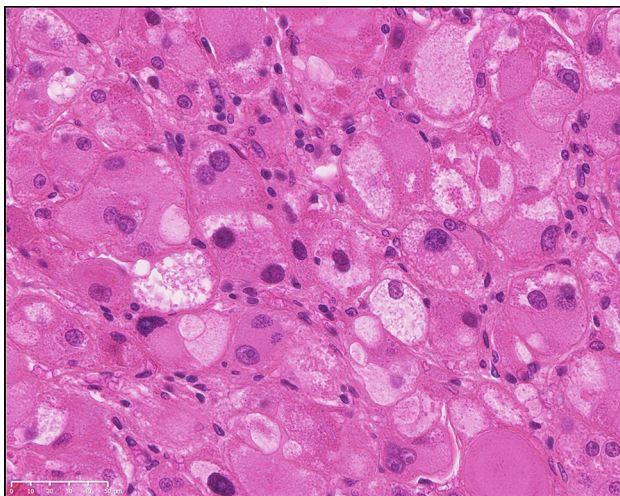


Fig. 7 Microphotograph of subtype 4 specificities, H&E staining magnification $\times 400$. Oncocytic cells possess an abundant, granular, eosinophilic cytoplasm with a round, nucleolated, eccentric nucleus. They are larger than compact eosinophilic cells. Anisokaryosis and anisocytosis are often marked

Specifically, in subtype 1, DAB2 stained trabeculae of cylindrical eosinophilic cells with no co-expression of CYP11B2. Specifically, in subtype 2, alpha inhibin was strongly expressed in compact cells and KDM1A immunoreexpression was weaker in the nodules than in the adjacent normal parenchyma.

Genetic Characteristics

Among the 35 patients in the series, 15 (43%) had a constitutional pathogenic *ARMC5* variant, 4 (11%) had a constitutional pathogenic *KDM1A* variant, and 16 (46%) had no specific or recurrent known pathological variant to date. No patient had a *PRKARIA*, *PRKACA*, *APC*, or *MEN1* pathological variant. *FH* pathogenic variants were not investigated as no patient had clinical suspicion of *FH* genetic alteration.

Correlations

BMI was significantly higher in subtype 1 patients than in patients from subtype 4. Plasma cortisol at 8:00 am in subtype 2 patients was significantly lower than in the other groups. No significant difference was found in the intensity

Table 6 Main characteristics of BMAD subtypes

	Subtype 1	Subtype 2	Subtype 3	Subtype 4
Round fibrous septa within macronodules	Yes	Yes	No	No
Clear cells	70 to 90%	60 to 70%	>90%	20 to 60%
Compact cells	10 to 30%	30 to 40%	<10%	<10%
Oncocytic cells	<10%	<10%	<10%	40 to 80%

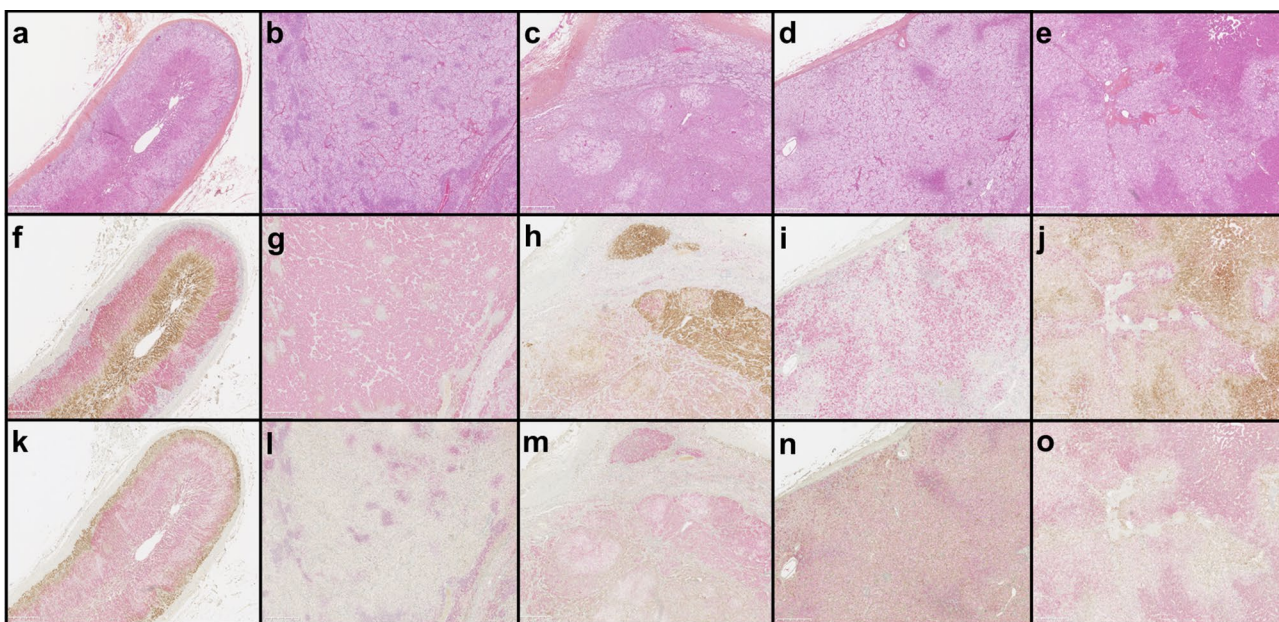


Fig. 8 H&E magnification×100 (a–e). Immunohistochemistry, double staining with HSD3B2 (red) and alpha-inhibin (brown) magnification×100 (f–j). Immunohistochemistry, double staining with DAB2 (brown), and CYP17A1 (red) magnification×100 (k–o). Normal adrenal gland (a, f, k); subtype 1 (b, g, l); subtype 2 (c, h, m); subtype 3 (d, i, n) subtype 4 (e, j, o). In all subtypes, HSD3B2 was preferentially

expressed by clear cells and CYP17A1 was preferentially expressed by compact eosinophilic cells. In most subtype 1 cases, HSD3B2 was expressed by all clear cells. In other subtypes, HSD3B2 was mainly heterogeneous on clear cells. In subtype 2 cases, alpha inhibin expression by compact cells was stronger than in other subtypes

of 24 h free urinary cortisol. On the CT scan, we found only one significant difference: the spontaneous adrenal density of subtype 4 was higher than in the other groups. The adrenal

size of subtype 4 was significantly smaller than in the other subtypes (Table 7). Type II correlated with the presence of a pathogenic *ARMC5* variant ($p < 0.01$). This criterion had

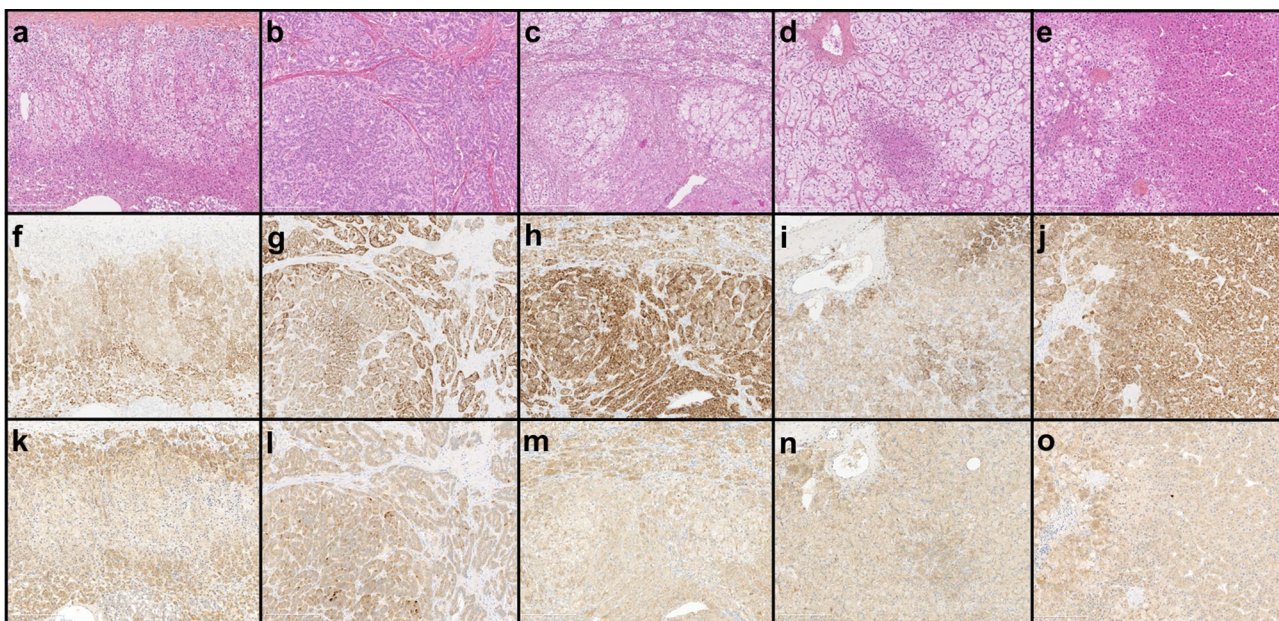


Fig. 9 H&E magnification×100 (a–e). Immunohistochemistry CYP11B1 magnification×100 (f–j), immunohistochemistry HSD3B1 magnification×100 (k–o). Normal adrenal gland (a, f, k); subtype 1 (b, g, l); subtype

2 (c, h, m); subtype 3 (d, i, n); subtype 4 (e, j, o). In all subtypes, both CYP11B1 and HSD3B1 were expressed by all cell types in all subtypes

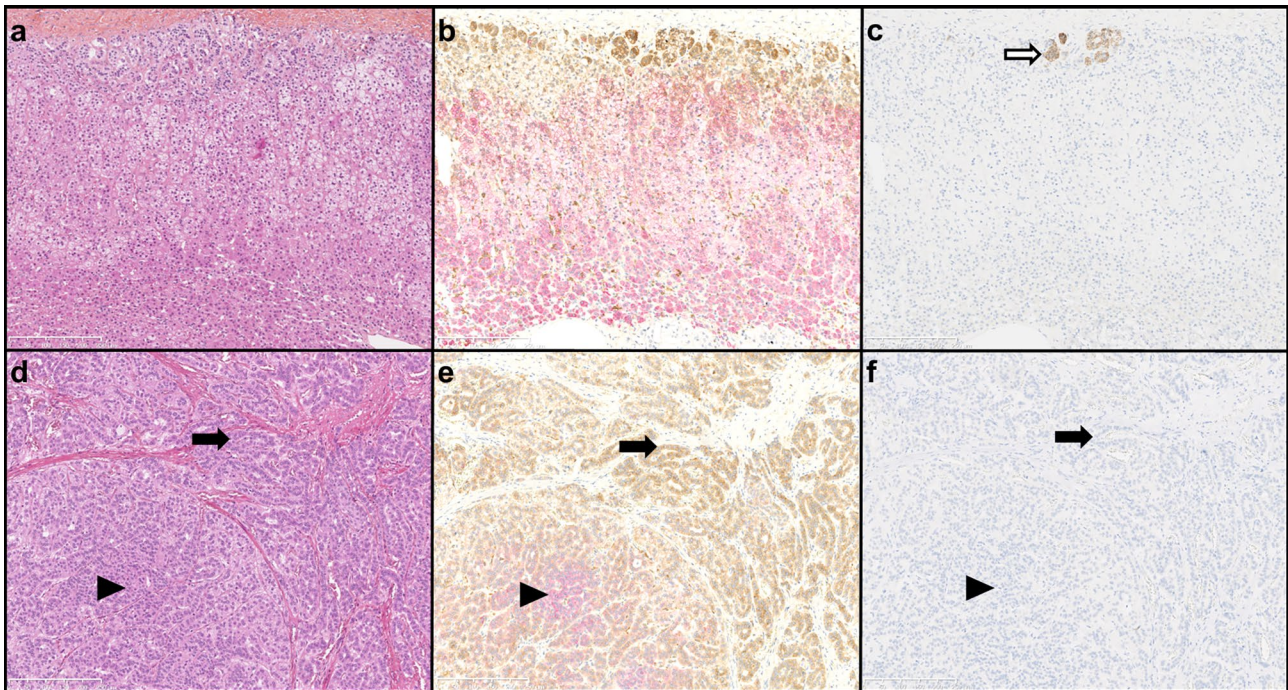


Fig. 10 H&E magnification $\times 100$ (a, d), double staining with DAB2 (brown) and CYP17A1 (red) magnification $\times 100$ (b, e). Immunohistochemistry CYP11B2 magnification $\times 100$ (c, f). Normal adrenal gland (a–c) zona fasciculata and reticularis express CYP17A1. Zona glomerulosa express DAB2. Within zona glomerulosa, some aldosterone-

producing cells express CYP11B2 (white arrow). In subtype 1 (d–f), islands of polygonal compact cells expressed CYP17A1 (arrowhead). Trabeculae of cylindrical eosinophilic cells expressed DAB2 (black arrow) with no expression of CYP11B2

a positive predictive value of 62.5% and a negative predictive value of 91.5% to detect a pathogenic *ARMC5* variant.

We analyzed the correlation between the morphological subtype and the genetic profile of the patients. Subtype 1

contained most patients with a constitutional pathogenic *ARMC5* variant. Subtype 2 contained exclusively patients with a constitutional pathogenic *KDM1A* variant. Subtypes

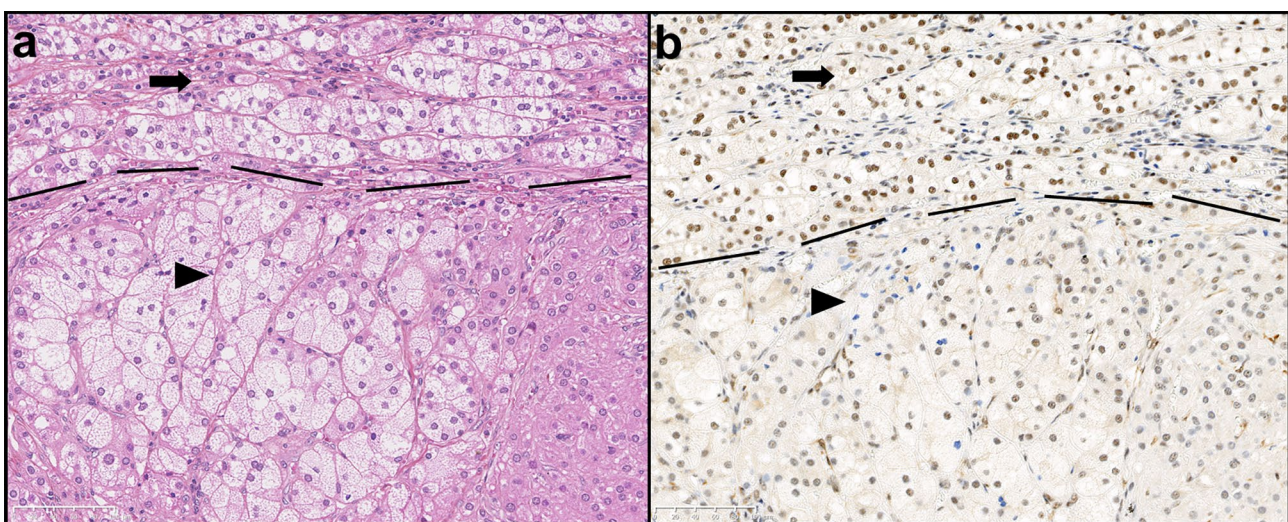


Fig. 11 H&E (a) and KDM1A immunohistochemistry (b) magnification $\times 200$. KDM1A expression is weaker in the nodules (arrowhead) compared to adjacent adrenal tissue (arrow)

Table 7 Correlation between clinical, biological, radiologic, genetic data, and morphological subtypes

Subtype characteristics ^a	Subtype 1	Subtype 2	Subtype 3	Subtype 4	p ^b
Sex					
Female	11	4	5	3	> 0.05
Male	7	0	3	2	
Age (year)	43	42	46	59	> 0.05
BMI	32.5	26.2	27.7	24	0.006*
Adrenalectomy					
Unilateral	4	1	6	2	> 0.05
Bilateral	14	3	2	3	
Adrenal gland size (mm)	99.2	83.8	106	62.3	0.03*
HU without IV	8.3	7	-2.3	23	0.02*
Constitutional genetic variant					
<i>ARMC5</i>	14	0	1	0	< 0.0001*
<i>KDM1A</i>	0	4	0	0	
Unknown	3	0	8	5	

^aQuantitative data are presented in means and qualitative data are presented in numbers

^bComparison between the 4 subtypes

3 and 4 mainly concerned patients without a known constitutional variant (Table 7).

The clear cells of the 15 patients with an *ARMC5* pathogenic variant uniformly express HSD3B2 in contrast to the 4 patients with a *KDM1A* pathogenic variant and 15 patients with no known genetic cause who express HSD3B2 heterogeneously on clear cells. Weak *KDM1A* expression in nodule cells was only seen in the 4 patients with a *KDM1A* pathogenic variant.

Discussion

We report here the first detailed pathological and exhaustive immunohistochemical description of a cohort of 35 patients with BMAD operated by unilateral or bilateral adrenalectomy in our center. In agreement with the literature, the majority of BMAD cases were female and the patients were mainly in their 6th decade when they underwent surgery [7, 11, 64, 65].

The microscopic characteristics found in our series were used to perform an unsupervised multiple-factor analysis. It separated the 35 patients into four distinct histopathological subtypes according to the presence of round fibrous septa and the proportion of cell types (clear, compact, oncocytic).

These morphological subtypes show a strong correlation with the genetic data of our cohort. Patients with a biallelic inactivation of *ARMC5* and *KDM1A* gene belong to two different microscopically homogeneous groups, subtype 1 and subtype 2, respectively. In contrast, patients without a known constitutional variant are morphologically heterogeneous and are distributed between subtypes 1, 3, and 4. All nodules of a patient have the same morphology. Type II was

more frequent in patients with a pathological *ARMC5* variant. These data strongly support the hypothesis of a causal link between the driver genes and the morphologic appearance of the adrenal glands in BMAD.

In the literature, the microscopic description of the 55 case reports of BMAD is very similar from one publication to another (Table 8). In most of the case reports, the microscopic description is unfortunately not sufficiently detailed to allow classification of the case according to our model. In our series, fibrous septa are frequent within macronodules but were only mentioned in one case report [18]. The presence of cylindrical eosinophilic cell trabeculae at the periphery of the nodules has only been described in one case [17]. To our knowledge, the presence of oncocytic cells has never been mentioned in the microscopic characteristics, and we found them in 5 out of 35 patients. The presence of myelolipomatous territories was reported in two cases [1, 44] and in some patients of a series of BMAD with pathological *KDM1A* variant [55].

In BMAD, the two main cell populations (clear and compact) have been studied by several authors, in particular, Sasano et al., using antibodies against steroidogenic enzymes involved in the synthesis of adrenal steroid hormones, in particular: HSD3B2 and CYP17A1 [66]. HSD3B2 is predominantly expressed in clear cells while CYP17A1 is preferentially expressed in compact eosinophilic cells [20, 21, 23, 25, 31, 34, 39]. Our immunohistochemical results, consistent with those previous observations, reinforce that this preferential staining of HSD3B2 in clear cells and CYP17A1 in compact cells as previously described by Sasano et al. [39] may become a diagnostic criterion of BMAD. Indeed, the lack of HSD3B2 and CYP17A1 co-expression may allow to distinguish BMAD from multiple cortisol-producing

Table 8 The microscopic description of the 55 case reports

Year	Author	Journal	Number of case	Age	Sex	Macroscopic description	Weight	Nodules size	Colour	Microscopic description	Adjacent cortex
1964	Kirschner	J Clin Endocrinol	1	40	F	numerous nodules	50 and 44 g	0.2 to 3.5 cm	bright yellow	cells similar to the zona fasciculata, and nests of smaller cells with granular eosinophilic cytoplasm	compressed
1975	Hidai	Endocrinol Japon	1	47	M	diffusely enlarged	105 and 56 g	NS	yellowish brown	similar to zona fasciculata	not visible
1977	Ishihara	Endocrinol Japon	1	51	M	multinodular mass	141 and 85 g	Up to 2-3 cm	yellowish white	round lipid-rich cells and smaller cells in the periphery	not visible
1980	Krivitzky	Ann med int	1	39	F	increased volume	30 and 80 g	NS	yellow ocre	spongiocytic cells	not visible
1983	Kawamura	Endocrinol Japon	1	47	F	swollen, multiple nodules	44 and 70 g	NS	yellowish	clear cell rich in lipid and darker cells	NS
1986	Hashimoto	Endocrinol Japon	1	51	M	enlarged multinodular mass bilateral	76 and 54 g	0.5 to 4 cm	yellowish	mainly clear cells and partly of compact cells	normal or compressed
1989	Cugini	Endocrinol Japon	1	48	M	giant with a grossly nodular surface	450 g each (necropsy)	NS	NS	cells with a clear cytoplasm	no atrophy
1989	Makino	Endocrinol Japon	1	51	M	multi-nodular adrenal masses	105 and 45 g	NS	yellow	clear cells	atrophy
1989	Malchoff	J Clin Endocrinol	1	47	M	multiple macronodules	62 and 24 g	NS	NS	large cells clear cytoplasm, less smaller cells	NS
1991	Aiba	Am J of Clin Pathol	4	51	M	bilateral enlargement	94 and 82 g	NS	yellow in all instance	clear cells and compact cells in limited number	atrophy
				52	M	bilateral enlargement	58 and 58 g	NS	yellow in all instance	clear cells and compact cells in limited number	not visible
				45	M	bilateral enlargement	83 and 40 g	NS	yellow in all instance	clear cells and compact cells in limited number	atrophy
				37	M	bilateral enlargement	57 and 15 g	NS	yellow and dark brown	clear cells and compact cells in limited number	atrophy
1991	Zeiger	Surgery	3	49	F	enlargement and lobulated aspect	52 g mean	0.5 to 3 cm	yellow	variable proportion of clear and compact cells	not visible
				51	F	enlargement and lobulated aspect	52 g mean	0.5 to 3 cm	yellow	variable proportion of clear and compact cells	not visible
				61	M	enlargement and lobulated aspect	52 g mean	0.5 to 3 cm	yellow	variable proportion of clear and compact cells	not visible
1992	Lacroix	NEJM	1	48	F	multiple nodules	35 and 20 g	1.4 to 2.8 cm	NS	acidophilic cuboidal cells	hyperplasia
1994	Koizumi	Endocrine journal	1	55	F	numerous nodules	105 and 95 g	NS	yellow	Cells with abundant clear cytoplasm, and less smaller cells	NS
1994	Lieberman	European J of Endocrinol	1	49	M	multinodular	199 and 93 g	up to 2 cm	yellow to tan	lipid-filled adrenocortical cells	no atrophy
1994	Sasano	Modern pathol	6	45	F	numerous nodules	70 and 55 g	NS	bright yellow	cells with clear cytoplasm and a variable number of compact cells	atrophy

Table 8 (continued)

Year	Author	Journal	Number of case	Age	Sex	Macroscopic description	Weight	Nodules size	Colour	Microscopic description	Adjacent cortex
				62	F	numerous nodules	80 and 104 g	NS	bright yellow	cells with clear cytoplasm and a variable number of compact cells	atrophy
				54	F	numerous nodules	95 and 105 g	NS	bright yellow	cells with clear cytoplasm and a variable number of compact cells	not visible
				52	M	numerous nodules	70 and 90 g	NS	bright yellow	cells with clear cytoplasm and a variable number of compact cells	atrophy
				60	M	numerous nodules	35 and 28 g	NS	bright yellow	cells with clear cytoplasm and a variable number of compact cells	not visible
				65	M	numerous nodules	34 and 46 g	NS	bright yellow	cells with clear cytoplasm and a variable number of compact cells	not visible
1995	Murakami	Intern med	2	45	F	bilateral adrenal mass	46 and 44 g	NS	NS	clear cells and some nests of compact cells	NS
				48	M	bilateral adrenal mass	20.5 and 27.8 g	NS	NS	clear cells and some nests of compact cells	NS
1995	Nemoto	Intern med	1	68	M	bilateral nodular enlargement	28 and 64 g	0.5 to 4 cm	yellow	clear cells resembling those of the zona fasciculata	compressed
1996	Wada	European J of Endocrinol	2	57	M	bilaterally enlarged adrenals	80 and 39 g	few mm to 3 cm	yellow	large clear cortical cells and small compact cells	NS
				35	M	bilaterally enlarged adrenals	52 and 10 (partial) g	few mm to 1.5 cm	yellow	large clear cortical cells and small compact cells	NS
1997	Tamura	Intern med	1	48	F	bilateral adrenal tumors	6.8 and 5.8 g	3.5 and 2.4 cm	brown	mainly compact cells right, mainly clear cells left	NS
1997	Terzolo	J Endocrinol Invest	2	44	M	huge enlargement of both adrenal glands	77 and 90 g	NS	yellow	clear cells with grossly vacuolated cytoplasm, some areas of smaller granular eosinophilic cells (5%)	not visible
1997	Yamada	Intern med	1	48	M	bilaterally enlarged multinodular adrenal gland	90 and 55 g	NS	yellow	clear cells with grossly vacuolated cytoplasm, some areas of smaller granular eosinophilic cells (15%)	atrophy
1998	Hayashi	Endocrine journal	1	74	F	both glands were enlarged with several nodules (necropsy)	40 and 10 g (subtotal) 70.4 and 39.5 g (necropsy)	NS	yellow	clear and granular cells	atrophy
1998	Swain	Arch Surg	9	51	F	bilateral adrenal nodules	3.1 and 13.6 g	up to 3.1 cm	NS	clear and compact cells	atrophy

Table 8 (continued)

Year	Author	Journal	Number of case	Age	Sex	Macroscopic description	Weight	Nodules size	Colour	Microscopic description	Adjacent cortex
				46	F	bilateral adrenal nodules	40 and 34 g	up to 3.5 cm	NS	clear and compact cells	atrophy
				40	F	bilateral adrenal nodules	7.6 and 10.3 g	up to 2.2 cm	NS	clear and compact cells	atrophy
				69	F	bilateral adrenal nodules	12 and 7.6 g	up to 4 cm	NS	clear cells	atrophy
				68	M	bilateral adrenal nodules	40 and 82 g	up to 2 cm	NS	clear and compact cells	atrophy
				55	F	bilateral adrenal nodules	47 and 100 g	up to 2.5 cm	NS	clear cells	atrophy
				51	M	bilateral adrenal nodules	101 and 117 g	up to 4.2 cm	NS	clear cells	atrophy
				58	F	bilateral adrenal nodules	22 and 25 g	up to 3.5 cm	NS	clear cells	atrophy
				68	F	bilateral adrenal nodules	75 and 85 g	up to 3.5 cm	NS	clear cells	atrophy
2005	Matyakhina	JCEM	1	HLRCC	F	several nodules on both glands	57.4 and 48 g	NS	NS	clear cells	NS
2006	Hsieh	J intern med	1	53	F	nodular enlargement of both glands	110 and 48 g	up to 2.5 cm	golden yellow	predominant clear cells	NS
2006	Kubo	Surg today	1	73	F	large bilateral adrenal glands with multiple nodules	48.5 and 39.2 g	NS	golden yellow	hyperplastic clear cells	NS
2006	Sato	Endocrine J	1	53	F	bilaterally enlarged adrenal glands with multiple nodules	75 g (unilat)	up to 4.5 cm	yellow	clear cells	NS
2011	Hayakawa	Intern med	1	52	M	adrenal mass with multiple nodules	NS	few mm to 4 cm	yellow	large clear cells	NS
2012	Kobayashi	Intern med	1	75	F	multiple nodules	21 g and NS	NS	yellow	clear cells with insular pattern compact cells	NS
2014	Rhee	KJIM	1	50	M	bilateral macronodules	NS	up to 4 cm	golden yellow	clear cells similar to those of the normal fasciculata layer	NS
2017	Tokumoto	BMC surgery	1	56	M	bilateral nodular masses	30 g (unilat)	NS	yellow	large clear cells and small compact cells	NS
2018	Jin	J med case reports	1	52	F	multinodular glands	NS	NS	golden yellow	predominant fascicular cells	NS
2020	Higashitani	Endocrinol diab and metabol	1	62	M	multiple nodules	NS	0.2 to 0.7 cm	golden yellow	mainly clear cells	NS
2021	He	BMC med genomic	1	51	M	bilateral enlargement of adrenal glands	NS	over 1 cm	yellow	hyperplasia of zona fasciculata	NS

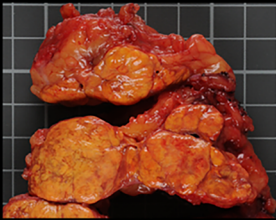

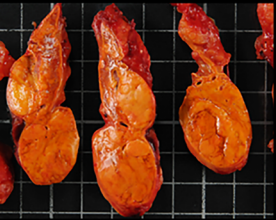
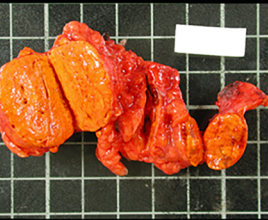
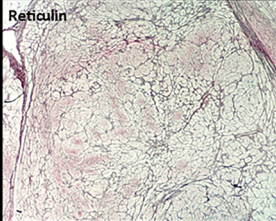
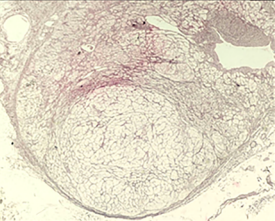
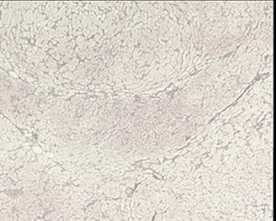
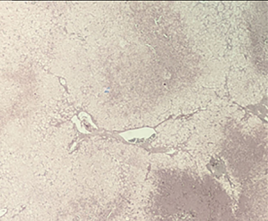
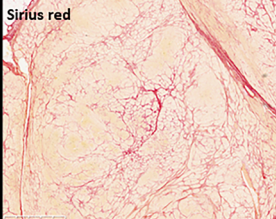
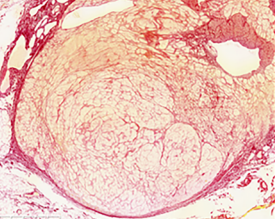


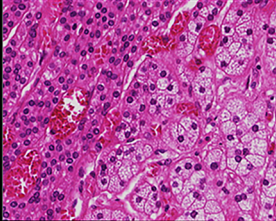
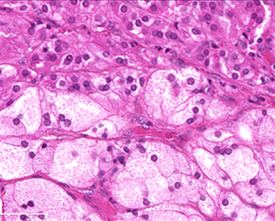
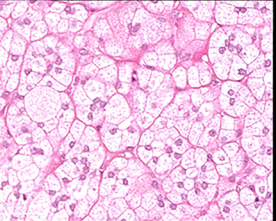
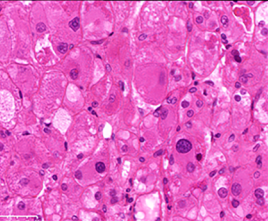
	Subtype 1	Subtype 2	Subtype 3	Subtype 4
Macroscopy				
	No residual adrenal	Residual adrenal	Residual adrenal	Residual adrenal
Architecture				
				
Microscopy				
	Clear cells: 70 to 90% Compact cells: 10 to 30% Oncocytic cells: < 10%	Clear cells: 60 to 70% Compact cells: 30 to 40% Oncocytic cells: <10%	Clear cells: > 90% Compact cells: < 10% Oncocytic cells: <10%	Clear cells: 20 to 60% Compact cells: < 10% Oncocytic cells: 40 to 80%
HSD3B2	Clear cells: frequently homogeneous Compact cells: -	Clear cells: heterogeneous Compact cells: -	Clear cells: heterogeneous Rarely homogeneous Compact cells: -	Clear cells: heterogeneous Compact cells: -
CYP17A1	Clear cells: - Compact cells: +	Clear cells: - Compact cells: +	Clear cells: - Compact cells: +	Clear cells: - Compact cells: +
Genetic	Frequent <i>ARMC5</i> alteration	<i>KDM1A</i> alteration	Rare <i>ARMC5</i> alteration	No known genetic alteration

Fig. 12 Graphical abstract of the main observations

adenomas (characterized by the co-expression of HSD3B2 and CYP17A1) [59, 67].

BMAD cells produce less cortisol than the normal adrenal gland cells, and hypercortisolism is due to the increase of the number of adrenal cells [68]. Sasano et al. postulated that this low efficiency of cortisol production could be explained by the lack of co-expression of HSD3B2 and CYP17A1. According to this hypothesis, as the different enzymatic steps of steroidogenesis would be performed in different cells, the efficiency of cortisol production would be decreased [39]. Our observations corroborate this hypothesis. We observed that the clear cells of patients with an *ARMC5* pathogenic variant uniformly express HSD3B2 in contrast to all other BMAD expressing HSD3B2 heterogeneously. Diffuse HSD3B2 expression could then explain, at least in part, the greater severity of Cushing's syndromes in *ARMC5* mutated patients compared to other BMAD patients [65]. HSD3B1 is expressed by all BMAD nodular cells. It is likely that this isoform of the enzyme, expressed in peripheral tissues, is not sufficient to replace HSD3B2. In conclusion, the partial expression of steroidogenic enzymes observed in BMAD nodule cells may participate to the reduction of cortisol production efficiency.

DAB2, a zona glomerulosa marker distinguishes the two populations of eosinophilic cells observed in subtype 1. The population of cylindrical eosinophilic cells in trabeculae at the periphery expressed DAB2 and did not express CYP11B2 or CYP17A1, whereas the population of compact eosinophilic cells in islands and bands expressed CYP17A1 and not DAB2. None of them appear to be able to produce aldosterone. Consistently, we did not find a correlation between subtype 1 and mineralocorticoid secretion (data not shown). Although hypertension is more frequent in *ARMC5* mutated patients than in the other BMAD groups [65], our immunohistochemical and biological data do not support the hypothesis of an aldosterone co-secretion explaining the hypertension in these patients.

Alpha inhibin had never been studied in BMAD to our knowledge. This marker is more expressed in compact cells of subtype 2 compared to other subtypes but we did not find a significant correlation between this subtype and androgen secretion (data not shown). Furthermore, previous studies showed that patients with a biallelic *KDM1A* inactivation have an overexpression of LH receptors on the surface of adrenal cells [55]. We can hypothesize that the high expression of alpha inhibin comparatively to the other subtypes leads to the inhibition of LH-FSH secretion in this group and then, activates a compensatory mechanism through overexpression of the LH receptor [69]. As observed before in a recent work from our group, weak expression of *KDM1A* in the nodules is a strong argument in favor of a *KDM1A* pathogenic variant [50].

The identification of these morphological and immunohistochemical correlations with genetics could have an impact on the genetic sequencing strategy of BMAD specimens from patients who underwent surgery. Patients with a pathogenic *ARMC5* variant frequently presented a type II and a microscopic subtype 1. All of them had a diffuse immunoeexpression of HSD3B2 on clear cells unlike other patients. Similarly, all patients with a pathological *KDM1A* variant had a microscopic subtype 2 phenotype and a weak immunoeexpression of *KDM1A* in the nodules compared to the adjacent adrenal gland. Because of their strong correlation with genetic clusters, the pathological characteristics could be incorporated into a genetic search strategy to target either *ARMC5* or *KDM1A* sequencing in adrenal specimens. We previously showed that in the presence of several bilateral nodules on CT scan and a plasma cortisol greater than 50 nmol/L after 1 mg of dexamethasone, the probability of carrying an *ARMC5* pathogenic variant is 20% with a sensitivity of 100% [65]. Pathology could guide the identification of this 20% subgroup of *ARMC5* mutated patients.

The main observations of this study are summarized in Fig. 12.

In conclusion, our study proposes the first histopathological classification of BMAD into 4 morphological subtypes based on the architecture of the macronodules and the proportion of cell types: clear, compact, and oncocyctic. This histopathological classification needs to be validated on a larger number of cases, but the strong correlation with the germinal genetic characteristics of the patients appears as a solid element of validation. This model highlights the heterogeneity of the pathological characteristics of BMAD as well as their link with the genetic characteristics.

Acknowledgements The authors would like to thank all the members of the department of pathology, Cochin Hospital, Paris, France, for their precious technical support.

Author Contribution F.V. and M.S. wrote the main manuscript text. F.V. L.B. M.B. and M.S. collected the data. All authors reviewed the manuscript.

Funding This work was supported by the Fondation pour la Recherche Médicale (EQU201903007854) and by the Agence Nationale de la Recherche (18-CE14-0008–01). FV and LB received a fellowship from ARC (association de recherche contre le cancer) foundation and from the CARPEM (Cancer research for personalized medicine). FV received a fellowship from FIREENDO (Filière maladies rares endocriniennes).

Availability of Data and Materials Not applicable.

Declarations

Ethical Approval All patients gave their written consent for research purposes including genetic analysis in the national COMETE network. This project was approved as a monocentric retrospective study by the data protection office (bureau de la protection des données, registre d'enregistrement AP-HP) (number 20220221155734) and the CLEP,

(comité local d'éthique des publications de l'hôpital Cochin) (number AAA-2022-08019). It complies with the principles of the declaration of Helsinki.

Competing Interests The authors declare no competing interests.

References

- Kirschner MA, Powell RD, Lipsett MB (1964) Cushing's Syndrome: Nodular Cortical Hyperplasia of Adrenal Glands with Clinical and Pathological Features Suggesting Adrenocortical Tumor. *J Clin Endocrinol Metab* 24:947–955. <https://doi.org/10.1210/jcem-24-10-947>
- Pakbaz S, Mete O (2019) Adrenal cortical neoplasia: from histology to molecular biology. *Diagnostic Histopathology* 25:178–189. <https://doi.org/10.1016/j.mpdhp.2019.02.004>
- Hodgson A, Pakbaz S, Mete O (2019) A Diagnostic Approach to Adrenocortical Tumors. *Surgical Pathology Clinics* 12:967–995. <https://doi.org/10.1016/j.path.2019.08.005>
- Juhlin CC, Bertherat J, Giordano TJ, Hammer GD, Sasano H, Mete O (2021) What Did We Learn from the Molecular Biology of Adrenal Cortical Neoplasia? From Histopathology to Translational Genomics. *Endocr Pathol* 32:102–133
- Mete O, Erickson LA, Juhlin CC, de Krijger RR, Sasano H, Volante M, Papotti MG (2022) Overview of the 2022 WHO Classification of Adrenal Cortical Tumors. *Endocr Pathol* 33:155–196. <https://doi.org/10.1007/s12022-022-09710-8>
- Lacroix A (2009) ACTH-independent macronodular adrenal hyperplasia. *Best Pract Res Clin Endocrinol Metab* 23:245–259. <https://doi.org/10.1016/j.beem.2008.10.011>
- Bouys L, Chiodini I, Arlt W, Reincke M, Bertherat J (2021) Update on primary bilateral macronodular adrenal hyperplasia (PBMAH). *Endocrine* 71:595–603. <https://doi.org/10.1007/s12020-021-02645-w>
- Zhang Q, Xiao H, Zhao L, et al (2020) Analysis of clinical and pathological features of primary bilateral macronodular adrenocortical hyperplasia compared with unilateral cortisol-secreting adrenal adenoma. *Ann Transl Med* 8:1173–1173. <https://doi.org/10.21037/atm-20-5963>
- Lefebvre H, Duparc C, Prévost G, Bertherat J, Louiset E (2015) Cell-To-Cell Communication in Bilateral Macronodular Adrenal Hyperplasia Causing Hypercortisolism. *Front Endocrinol*. <https://doi.org/10.3389/fendo.2015.00034>
- Lacroix A, Bourdeau I, Lampron A, Mazucco TL, Tremblay J, Hamet P (2009) Aberrant G-protein coupled receptor expression in relation to adrenocortical overfunction. *Clinical Endocrinology*. <https://doi.org/10.1111/j.1365-2265.2009.03689.x>
- Stratakis CA (2009) New genes and/or molecular pathways associated with adrenal hyperplasias and related adrenocortical tumors. *Mol Cell Endocrinol* 300:152–157. <https://doi.org/10.1016/j.mce.2008.11.010>
- Hsiao H-P, Kirschner LS, Bourdeau I, et al. (2009) Clinical and Genetic Heterogeneity, Overlap with Other Tumor Syndromes, and Atypical Glucocorticoid Hormone Secretion in Adrenocorticotropin-Independent Macronodular Adrenal Hyperplasia Compared with Other Adrenocortical Tumors. *J Clin Endocrinol Metab* 94:2930–2937. <https://doi.org/10.1210/jc.2009-0516>
- Hidai H, Fujii H, Otsuka K, Abe K, Shimizu N (1975) Cushing's Syndrome due to Huge Adrenocortical Multinodular Hyperplasia. *Endocrinol Jpn* 22:555–560. <https://doi.org/10.1507/endocrj1954.22.555>
- Hashimoto K, Kawada Y, Murakami K, et al (1986) Cortisol responsiveness to insulin-induced hypoglycemia in Cushing's syndrome with huge nodular adrenocortical hyperplasia. *Endocrinol Jpn* 33:479–487. <https://doi.org/10.1507/endocrj1954.33.47915>
- Makino S, Hashimoto K, Sugiyama M, Hirasawa R, Takao T, Ota Z, Saegusa M, Ohashi T, Omori H (1989) Cushing's Syndrome Due to Huge Nodular Adrenocortical Hyperplasia with Fluctuation of Urinary 17-OHCS Excretion. *Endocrinol Jpn* 36:655–663. <https://doi.org/10.1507/endocrj1954.36.655>
- Cugini P, Battisti P, Palma LD, Sepe M, Kawasaki T, Uezono K, Sasaki H (1989) "GIANT" Macronodular Adrenal Hyperplasia Causing Cushing's Syndrome: Case Report and Review of the Literature on a Clinical Distinction of Adrenocortical Nodular Pathology Associated with Hypercortisolism. *Endocrinol Jpn* 36:101–116. <https://doi.org/10.1507/endocrj1954.36.101>
- Malchoff CD, Rosa J, Debold CR, et al. (1989) Adrenocorticotropin-Independent Bilateral Macronodular Adrenal Hyperplasia: An Unusual Cause of Cushing's Syndrome. *J Clin Endocrinol Metab* 68:855–860. <https://doi.org/10.1210/jcem-68-4-855>
- Aiba M, Hirayama A, Iri H, et al (1991) Adrenocorticotrophic Hormone—Independent Bilateral Adrenocortical Macronodular Hyperplasia as a Distinct Subtype of Cushing's Syndrome Enzyme Histochemical and Ultrastructural Study of Four Cases with a Review of the Literature. *Am J Clin Pathol* 96:334–340. <https://doi.org/10.1093/ajcp/96.3.334>
- Lacroix A, Bolté E, Tremblay J, et al (1992) Gastric Inhibitory Polypeptide-Dependent Cortisol Hypersecretion — A New Cause of Cushing's Syndrome. *N Engl J Med* 327:974–980. <https://doi.org/10.1056/NEJM199210013271402>
- Koizumi S, Beniko M, Ikota A, et al (1994) Adrenocorticotrophic Hormone-Independent Bilateral Adrenocortical Macronodular Hyperplasia: A Case Report and Immunohistochemical Studies. *Endocr J* 41:429–435. <https://doi.org/10.1507/endocrj.41.42921>
- Murakami O, Satoh F, Takahashi K, et al (1995) Three Cases of Clinical or Preclinical Cushing's Syndrome due to Adrenocorticotrophic Hormone-Independent Bilateral Adrenocortical Macronodular Hyperplasia: Pituitary-Adrenocortical Function and Immunohistochemistry. *Intern Med* 34:1074–1081. <https://doi.org/10.2169/internalmedicine.34.1074>
- Nemoto Y, Aoki A, Katayama Y, et al (1995) Non-Cushingoid Cushing's Syndrome due to Adrenocorticotrophic Hormone-Independent Bilateral Adrenocortical Macronodular Hyperplasia. *Intern Med* 34:446–450. <https://doi.org/10.2169/internalmedicine.34.446>
- Wada N, Kubo M, Kijima H, Ishizuka T, Saeki T, Koike T, Sasano H (1996) Adrenocorticotropin-independent bilateral macronodular adrenocortical hyperplasia: immunohistochemical studies of steroidogenic enzymes and post-operative course in two men. *Eur J Endocrinol* 134:583–587. <https://doi.org/10.1530/eje.0.1340583>
- Terzolo M, Boccuzzi A, Alí A, Bollito E, De Risi C, Paccotti P, Angeli A (1997) Cushing's syndrome due to ACTH-independent bilateral adrenocortical macronodular hyperplasia. *J Endocrinol Invest* 20:270–275. <https://doi.org/10.1007/BF03350299>
- Tamura H, Sugihara H, Minami S, et al (1997) Cushing's Syndrome due to Bilateral Adrenocortical Adenomas with Different Pathological Features. *Intern Med* 36:804–809. <https://doi.org/10.2169/internalmedicine.36.804>
- Hayashi Y, Takeda Y, Kaneko K, Koyama H, Aiba M, Ikeda U, Shimada K (1998) A Case of Cushing's Syndrome due to ACTH-Independent Bilateral Macronodular Hyperplasia Associated with Excessive Secretion of Mineralocorticoids. *Endocr J* 45:485–491. <https://doi.org/10.1507/endocrj.45.485>
- Swain JM, Grant CS, Schlinkert RT, Thompson GB, van Heerden JA, Lloyd RV, Young WF (1998) Corticotropin-Independent Macronodular Adrenal Hyperplasia: A Clinicopathologic Correlation. *Arch Surg*. <https://doi.org/10.1001/archsurg.133.5.541>
- Hsieh M-H, Chang C-C, Lin M-C, Chang T-C (2006) Adrenocorticotropin-Independent Bilateral Adrenal Macronodular Hyperplasia (AIMAH) A Case Report. *J Intern Med Taiwan*. 17:291–297

29. Kubo N, Onoda N, Ishikawa T, et al (2006) Simultaneous Bilateral Laparoscopic Adrenalectomy for Adrenocorticotrophic Hormone-Independent Macronodular Adrenal Hyperplasia: Report of a Case. *Surg Today* 36:642–646. <https://doi.org/10.1007/s00595-006-3209-6>
30. Sato M, Soma M, Nakayama T, et al (2006) A Case of Adrenocorticotropin-independent Bilateral Adrenal Macronodular Hyperplasia (AIMAH) with Primary Hyperparathyroidism (PHPT). *Endocr J* 53:111–117. <https://doi.org/10.1507/endocrj.53.111>
31. Hayakawa E, Yoshimoto T, Hiraishi K, Kato M, Izumiyama H, Sasano H, Hirata Y (2011) A Rare Case of ACTH-independent Macronodular Adrenal Hyperplasia Associated with Aldosterone-producing Adenoma. *Intern Med* 50:227–232. <https://doi.org/10.2169/internalmedicine.50.4351>
32. Kobayashi T, Miwa T, Kan K, et al (2012) Usefulness and Limitations of Unilateral Adrenalectomy for ACTH-independent Macronodular Adrenal Hyperplasia in a Patient with Poor Glycemic Control. *Intern Med* 51:1709–1713. <https://doi.org/10.2169/internalmedicine.51.7041>
33. Rhee H, Jeon YK, Kim SS, Kang YH, Son SM, Kim YK, Kim IJ (2014) Adrenocorticotrophic hormone-independent macronodular adrenal hyperplasia with abnormal cortisol secretion mediated by catecholamines. *Korean J Intern Med* 29:667. <https://doi.org/10.3904/kjim.2014.29.5.667>
34. Tokumoto M, Onoda N, Tauchi Y, et al (2017) A case of Adrenocorticotrophic hormone -independent bilateral adrenocortical macronodular hyperplasia concomitant with primary aldosteronism. *BMC Surg* 17:97. <https://doi.org/10.1186/s12893-017-0293-z>
35. Jin P, Janjua MU, Zhang Q, Dong C, Yang Y, Mo Z (2018) Extensive ARMC5 genetic variance in primary bilateral macronodular adrenal hyperplasia that started with exophthalmos: a case report. *J Med Case Reports* 12:13. <https://doi.org/10.1186/s13256-017-1529-3>
36. Higashitani T, Karashima S, Aono D, et al (2020) A case of renovascular hypertension with incidental primary bilateral macronodular adrenocortical hyperplasia. *Endocrinol Diabetes Metab Case Rep.* 6:19-0163. <https://doi.org/10.1530/EDM-19-0163>
37. He W-T, Wang X, Song W, et al (2021) A novel nonsense mutation in ARMC5 causes primary bilateral macronodular adrenocortical hyperplasia. *BMC Med Genomics* 14:126. <https://doi.org/10.1186/s12920-021-00896-0>
38. Matyakhina L, Freedman RJ, Bourdeau I, et al (2005) Hereditary Leiomyomatosis Associated with Bilateral, Massive, Macronodular Adrenocortical Disease and Atypical Cushing Syndrome: A Clinical and Molecular Genetic Investigation. *J Clin Endocrinol Metab* 90:3773–3779. <https://doi.org/10.1210/jc.2004-2377>
39. Sasano H, Suzuki T, Nagura H (1994) ACTH-independent macronodular adrenocortical hyperplasia: immunohistochemical and in situ hybridization studies of steroidogenic enzymes. *Mod Pathol* 7:215–219
40. Ishihara T, Uchihira F, Tatsumi M, Mori T, Igarashi T, Takayama H, Ishikawa T (1977) A Case with Cushing Syndrome Due to Huge Bilateral Adrenal Nodular Hyperplasia. *Folia Endocrinol* 53:1082–1093. https://doi.org/10.1507/endocrine1927.53.9_1082
41. Krivitzky A, Blondeau P, Camilleri JP, Delzant G, Roche-Sicot J (1980) [Cushing's syndrome caused by a bilateral adrenal adenoma (author's transl)]. *Ann Med Interne (Paris)* 131:361–364
42. Kawamura M, Shiraha S, Sudo T, et al (1983) A Case Of A Total Bilateral Adrenalectomy For Cushing's Syndrome Due To Bilateral Nodular Adrenocortical Hyperplasia. *The journal of the Japanese Practical Surgeon Society* 44:183–190. <https://doi.org/10.3919/ringe1963.44.183>
43. Zeiger MA, Nieman LK, Cutler GB, Chrousos GP, Doppman JL, Travis WD, Norton JA (1991) Primary bilateral adrenocortical causes of Cushing's syndrome. *Surgery* 110:1106–1115
44. Lieberman SA, Eccleshall TR, Feldman D (1994) ACTH-independent massive bilateral adrenal disease (AIMBAD): A subtype of Cushing's syndrome with major diagnostic and therapeutic implications. *European Journal of Endocrinology* 131:67–73. <https://doi.org/10.1530/eje.0.1310067>
45. Yamada Y, Sakaguchi K, Inoue T, et al (1997) Preclinical Cushing's Syndrome due to Adrenocorticotropin-Independent Bilateral Adrenocortical Macronodular Hyperplasia with Concurrent Excess of Gluco- and Mineralocorticoids. *Intern Med* 36:628–632. <https://doi.org/10.2169/internalmedicine.36.628>
46. Chevalier B, Vantghem M-C, Espiard S (2021) Bilateral Adrenal Hyperplasia: Pathogenesis and Treatment. *Biomedicines* 9:1397. <https://doi.org/10.3390/biomedicines9101397>
47. Skogseid B, Larsson C, Lindgren PG, Kvanta E, Rastad J, Theodorsson E, Wide L, Wilander E, Oberg K (1992) Clinical and genetic features of adrenocortical lesions in multiple endocrine neoplasia type 1. *J Clin Endocrinol Metab* 75:76–81. <https://doi.org/10.1210/jcem.75.1.1352309>
48. Langer P, Cupisti K, Bartsch DK, Nies C, Goretzki PE, Rothmund M, Röher HD (2002) Adrenal Involvement in Multiple Endocrine Neoplasia Type 1. *World J Surg* 26:891–896
49. Marchesa P, Fazio VW, Church JM, McGannon E (1997) Adrenal masses in patients with familial adenomatous polyposis. *Dis Colon Rectum* 40:1023–1028. <https://doi.org/10.1007/BF0205092348>
50. Vaczlavik A, Bouys L, Violon F, et al (2022) KDM1A inactivation causes hereditary food-dependent Cushing syndrome. *Genetics in Medicine* 24:374–383. <https://doi.org/10.1016/j.gim.2021.09.018>
51. Assié G, Rizk-Rabin M, Barreau O, Guignat L, René-Corail F, Poussier A, Borson-Chazot F, Bertagna X, Ragazzon B (2013) ARMC5 Mutations in Macronodular Adrenal Hyperplasia with Cushing's Syndrome. *N Engl J Med* 28:369(22):2105. <https://doi.org/10.1056/NEJMoa1304603>
52. Espiard S, Drouot L, Libé R, et al (2015) ARMC5 Mutations in a Large Cohort of Primary Macronodular Adrenal Hyperplasia: Clinical and Functional Consequences. *J Clin Endocrinol Metab* 100:E926–E935. <https://doi.org/10.1210/jc.2014-4204>
53. Bonnet-Serrano F, Bertherat J (2018) Genetics of tumors of the adrenal cortex. *Endocrine-Related Cancer* 25:R131–R152. <https://doi.org/10.1530/ERC-17-0361>
54. Drouot L, Espiard S, Bertherat J (2015) Genetics of primary bilateral macronodular adrenal hyperplasia: a model for early diagnosis of Cushing's syndrome? *European Journal of Endocrinology* 173:M121–M131. <https://doi.org/10.1530/EJE-15-0532>
55. Chasseloup F, Bourdeau I, Tabarin A, et al (2021) Loss of KDM1A in GIP-dependent primary bilateral macronodular adrenal hyperplasia with Cushing's syndrome: a multicentre, retrospective, cohort study. *Lancet Diabetes Endocrinol* 9:813–824. [https://doi.org/10.1016/S2213-8587\(21\)00236-9](https://doi.org/10.1016/S2213-8587(21)00236-9)
56. Volante M, Bollito E, Sperone P, et al (2009) Clinicopathological study of a series of 92 adrenocortical carcinomas: from a proposal of simplified diagnostic algorithm to prognostic stratification. *Histopathology* 55:535–543. <https://doi.org/10.1111/j.1365-2559.2009.03423.x>
57. Duregon E, Fassina A, Volante M, et al (2013) The Reticulin Algorithm for Adrenocortical Tumor Diagnosis: A Multicentric Validation Study on 245 Unpublished Cases. *American Journal of Surgical Pathology* 37:1433–1440. <https://doi.org/10.1097/PAS.0b013e31828d387b>
58. Huang Y, de Boer WB, Adams LA, MacQuillan G, Rossi E, Rigby P, Raftopoulos SC, Bulsara M, Jeffrey GP (2013) Image analysis of liver collagen using sirius red is more accurate and correlates better with serum fibrosis markers than trichrome. *Liver Int* 33:1249–1256. <https://doi.org/10.1111/liv.12184>
59. Kubota-Nakayama F, Nakamura Y, Konosu-Fukaya S, et al (2016) Expression of steroidogenic enzymes and their transcription factors in cortisol-producing adrenocortical adenomas: immunohistochemical analysis and quantitative real-time polymerase chain

- reaction studies. *Hum Pathol* 54:165–173. <https://doi.org/10.1016/j.humpath.2016.03.016>
60. Mete O, Asa SL, Giordano TJ, Papotti M, Sasano H, Volante M (2018) Immunohistochemical Biomarkers of Adrenal Cortical Neoplasms. *Endocr Pathol* 29:137–149. <https://doi.org/10.1007/s12022-018-9525-8>
61. Boulkroun S, Samson-Couterie B, Dzib J-FG, et al (2010) Adrenal Cortex Remodeling and Functional Zona Glomerulosa Hyperplasia in Primary Aldosteronism. *Hypertension* 56:885–892. <https://doi.org/10.1161/HYPERTENSIONAHA.110.158543>
62. Gomez-Sanchez CE, Gomez-Sanchez EP, Nishimoto K (2020) Immunohistochemistry of the Human Adrenal CYP11B2 in Normal Individuals and in Patients with Primary Aldosteronism. *Horm Metab Res* 52:421–426. <https://doi.org/10.1055/a-1139-2079>
63. Arola J, Liu J, Heikkilä P, Voutilainen R, Kahri A (1998) Expression of inhibin α in the human adrenal gland and adrenocortical tumors. *Endocrine Research* 24:865–867. <https://doi.org/10.3109/07435809809032699>
64. Christopoulos S, Bourdeau I, Lacroix A (2005) Clinical and Subclinical ACTH-Independent Macronodular Adrenal Hyperplasia and Aberrant Hormone Receptors. *Horm Res Paediatr* 64:119–131. <https://doi.org/10.1159/000088818>
65. Bouys L, Vaczlavik A, Jouinot A, et al (2022) Identification of predictive criteria for pathogenic variants of primary bilateral macronodular adrenal hyperplasia (PBMAH) gene ARMC5 in 352 unselected patients. *Eur J Endocrinol* 187:123–134. <https://doi.org/10.1530/EJE-21-1032>
66. Nishimoto K, Nakagawa K, Li D, et al (2010) Adrenocortical Zonation in Humans under Normal and Pathological Conditions. *J Clin Endocrinol Metab* 95:2296–2305. <https://doi.org/10.1210/jc.2009-2010>
67. Rege J, Hoxie J, Liu C-J, et al (2022) Targeted Mutational Analysis of Cortisol-Producing Adenomas. *J Clin Endocrinol Metab* 107:e594–e603. <https://doi.org/10.1210/clinem/dgab682>
68. Assie G, Louiset E, Sturm N, et al (2010) Systematic Analysis of G Protein-Coupled Receptor Gene Expression in Adrenocorticotropin-Independent Macronodular Adrenocortical Hyperplasia Identifies Novel Targets for Pharmacological Control of Adrenal Cushing's Syndrome. *J Clin Endocrinol Metab* 95:E253–E262. <https://doi.org/10.1210/jc.2009-2281>
69. Menon KMJ, Menon B (2014) Regulation of luteinizing hormone receptor expression by an RNA binding protein: role of ERK signaling. *Indian J Med Res* 140 Suppl:S112-119.

Publisher's Note Springer Nature remains neutral with regard to jurisdictional claims in published maps and institutional affiliations.

Springer Nature or its licensor (e.g. a society or other partner) holds exclusive rights to this article under a publishing agreement with the author(s) or other rightsholder(s); author self-archiving of the accepted manuscript version of this article is solely governed by the terms of such publishing agreement and applicable law.